Provided for non-commercial research and education use.
Not for reproduction, distribution or commercial use.

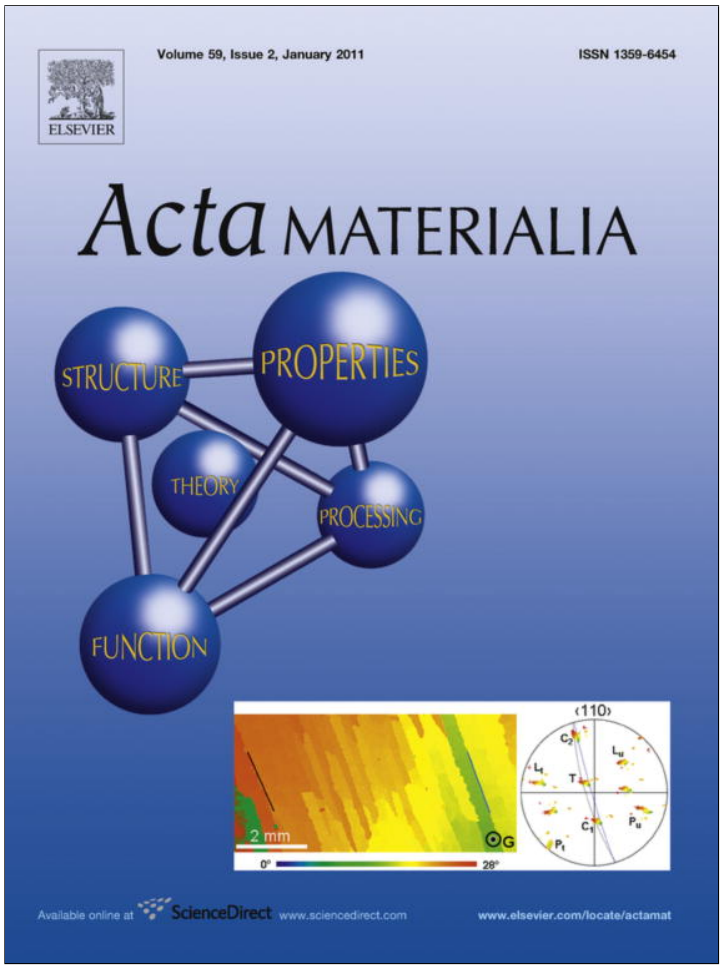

This article appeared in a journal published by Elsevier. The attached copy is furnished to the author for internal non-commercial research and education use, including for instruction at the authors institution and sharing with colleagues.

Other uses, including reproduction and distribution, or selling or licensing copies, or posting to personal, institutional or third party websites are prohibited.

In most cases authors are permitted to post their version of the article (e.g. in Word or Tex form) to their personal website or institutional repository. Authors requiring further information regarding Elsevier's archiving and manuscript policies are encouraged to visit:

http://www.elsevier.com/copyright

Author's personal copy

Available online at www.sciencedirect.com
ScienceDirect
Acta Materialia 59 (2011) 678–685
Acta MATERIALIA
www.elsevier.com/locate/actamat

Elongated nanoscale voids at deformed special grain boundary structures in nanocrystalline materials

I.A. Ovid'ko, A.G. Sheinerman *, N.V. Skiba

Institute of Problems of Mechanical Engineering, Russian Academy of Sciences, Bolshoj 61, Vasil. Ostrov, St. Petersburg 199178, Russia

Received 9 June 2010; received in revised form 1 October 2010; accepted 2 October 2010

Abstract

A special micromechanism for the formation of elongated nanoscale voids at grain boundaries (GBs) in deformed nanocrystalline materials is suggested and theoretically described. Within our description, the formation of nanoscale voids represents a slow (diffusion-controlled) process driven by release of the elastic energy of GB disclination configurations formed due to GB sliding. It is demonstrated that the nucleation of elongated nanoscale voids at GB disclination dipoles occurs as an energetically favorable process in deformed nanocrystalline Ni and Al_2O_3 (sapphire) in wide ranges of their parameters.
© 2010 Acta Materialia Inc. Published by Elsevier Ltd. All rights reserved.

Keywords: Nanocrystalline materials; Fracture; Ductility; Grain boundary defects; Disclinations

1. Introduction

Fracture processes in nanocrystalline materials (having superior strength and being of great interest with regard to a wide range of applications) are the subject of intensive experimental research [1–10], computer simulations [11–14] and theoretical examinations ([15–19]; see also [20–22,23]). Nanocrystalline materials exhibit either ductile or brittle fracture behavior, depending on their structural characteristics and the conditions of mechanical loading. For instance, there are nanocrystalline materials showing intergranular brittle fracture [2,3,8], where the main brittle crack is treated as forming through multiple generations of intergranular nano/microscale cracks and their convergence. At the same time, there are several experimental reports on nanocrystalline materials exhibiting ductile fracture with preceding neck formation and dimpled structures at fracture surfaces [1–7]. The dimpled fracture structures are often observed in nanocrystalline materials specified by very low degrees (around 2%) of overall plastic strain (see e.g. [24,25]). Though the macroscopic deformation behavior of such materials is very similar to that of conventional brittle solids, they show ductile fracture at the microscopic level. This combination of macroscopically low plasticity and microscopically ductile fracture with dimpled structures is the subject of intense debate [1,9,20,25,26] and is sometimes called a paradox [9]. The size of dimples in nanocrystalline materials is commonly considerably larger than the grain size, and ductile fracture is viewed to occur through the void nucleation and coalescence mechanism. With the role of voids being important in fracture processes in nanocrystalline materials, of utmost interest are the fundamental micromechanisms for deformation-induced formation of voids as carriers of ductile fracture and the competition between void formation and deformation-induced formation of brittle cracks serving as carriers of brittle fracture. Knowledge of both the fundamental micromechanisms and the competition in question could shed light on the combination of macroscopically low plasticity and microscopically ductile fracture in nanocrystalline materials.

In conventional coarse-grained polycrystals, formation of brittle cracks and nucleation of voids is strongly influenced by grain boundaries (GBs), which are thereby responsible for the effects of grain size on the mechanical

* Corresponding author.
E-mail address: shein77@mail.ru (A.G. Sheinerman).

1359-6454/$36.00 © 2010 Acta Materialia Inc. Published by Elsevier Ltd. All rights reserved.
doi:10.1016/j.actamat.2010.10.005

Author's personal copy

properties of such materials (see e.g. [27–30]). In particular, deformation-induced nucleation of voids is believed to occur as a process releasing high local stresses created by either lattice dislocation pile-ups stopped at GBs or GB dislocation pile-ups stopped at triple junctions and ledges of GBs [30]. When the grain size of a material decreases down to the nanometer scale, large pile-ups of GB and lattice dislocations – "dangerous" stress sources capable of initiating voids – hardly form due to geometric restrictions [23,31,32]. In these circumstances, one expects that specific micromechanisms (different from those operating in coarse-grained polycrystals) for deformation-induced formation of voids come into play in nanocrystalline materials, and these expectations are confirmed by experiments. For instance, in situ transmission electron microscopy (TEM) observations [33,34] of plastically deforming nanocrystalline Au films (with average grain sizes of around 8–10 nm) revealed the absence of bulk dislocation activity; instead, nanopore nucleation and growth at triple junctions of GBs was observed, followed by void coalescence and nanodamage development. Also, an in situ TEM experiment [1] revealed the formation of nanovoids at GBs and their triple junctions in deformed nanocrystalline Ni (with an average grain size of around 30 nm) showing good ductility.

To understand the nature of specific micromechanism(s) for deformation-induced formation of voids in nanocrystalline materials, of particular importance is the fact that, in parallel with conventional lattice dislocation slip, specific deformation modes operate in nanocrystalline materials [20,23]. One such deformation mode in nanocrystalline materials is GB sliding [20,23,32,35–37]. This mode produces GB disclination dipoles at and near triple junctions [17,19,38]. GB dipoles serve as stress sources capable of initiating the rapid formation of brittle nanocracks, carriers of brittle fracture in nanocrystalline materials [17,19,38]. We think that, in addition, GB disclination dipoles at triple junctions can initiate the slow (diffusion-controlled) formation of voids, carriers of viscous fracture in nanocrystalline materials. The main aim of this paper is to theoretically describe the formation of nanoscale voids at GB disclination dipoles, examine their energy characteristics and compare them with those in the formation of brittle nanocracks in nanocrystalline materials.

2. Formation of nanoscale voids at grain boundaries with disclination dipoles in nanocrystalline materials

Let us consider a nanocrystalline solid consisting of nanoscale grains divided by GBs. The solid is under a remote tensile load. A two-dimensional section of the solid is schematically shown in Fig. 1a. We examine the situation where GB sliding significantly contributes to plastic flow of the nanocrystalline solid. Such a situation is realized, in particular, during superplastic deformation of nanocrystalline materials [39]. Following Refs. [17,19,38], GB disclination dipoles typically form due to GB sliding. For instance,

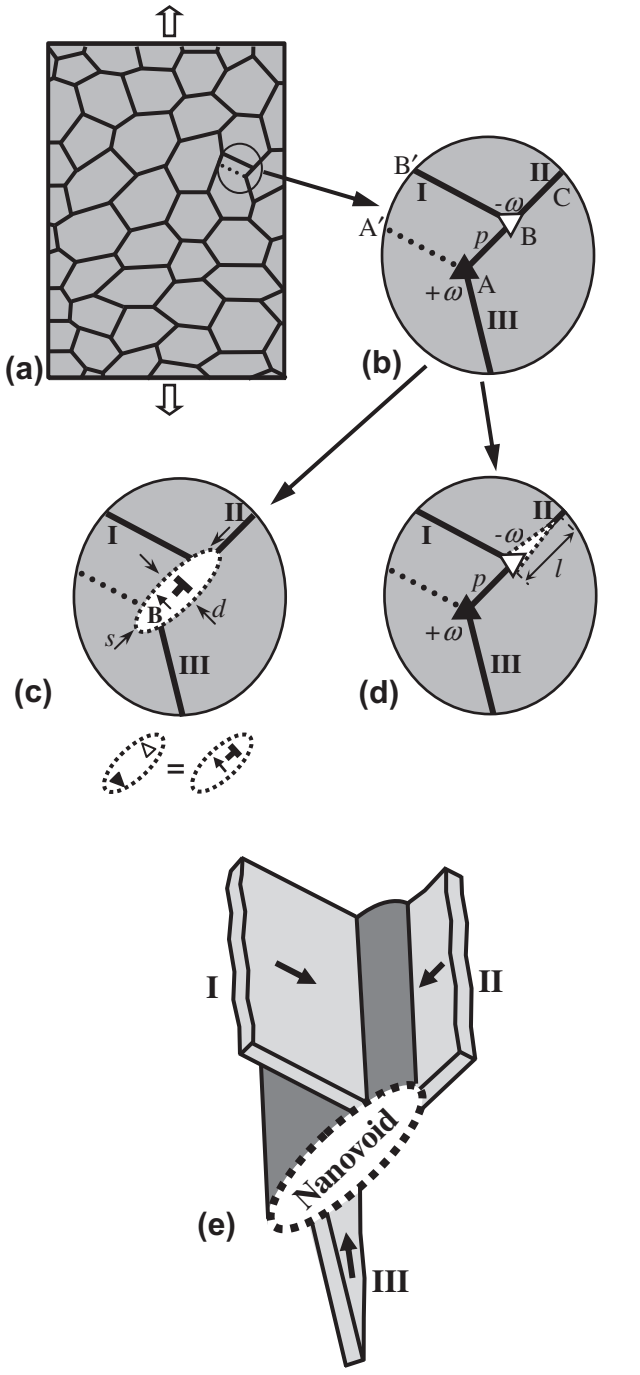

Fig. 1. Formation of an elliptic nanoscale void and a nanoscale brittle crack at a disclination dipole in nanocrystalline specimen deformed by grain boundary sliding. (a) General view. (b) Grain boundary sliding occurs along grain boundary II (AC) and results in the transfer of both grain boundary I (from position AA′ to position BB′) and the triple junction (from position A to position B) over the distance p. Also, a disclination dipole (with the distance p between the wedge disclinations) is generated in a nanocrystalline specimen due to grain boundary sliding. (c) An elliptic void with the axes s and d forms around the disclination dipole. In this case, the disclination dipole becomes equivalent to an edge dislocation. (d) A brittle nanoscale crack nucleates at one of the dipole disclinations. (e) A three-dimensional picture of the elliptic void that represents a "sheet-like structure" growing at the grain boundary interface and in its vicinity. Arrows show the directions of vacancy diffusion flows along grain boundaries towards the nanovoid.

Author's personal copy

Fig. 1b schematically shows the transfer of a high-angle tilt boundary I (from position AA′ to position BB′) due to GB sliding along the high-angle boundary II (AC). In the initial state, the triple junction A of high-angle GBs is supposed to be geometrically balanced. (There is no angle gap at the triple junction A; in other words, the sum of tilt misorientation angles at this triple junction is equal to zero.) As a result of transfer, the angle gaps ω and $-\omega$ appear at the GB junctions A and B, respectively (Fig. 1b), where ω is the tilt misorientation of the high-angle boundary I [18,40,41]. In the theory of defects in solids, the junctions A and B with the angle gaps $\pm\omega$ represent wedge disclinations which are characterized by the strengths $\pm\omega$ [42,43] and form a dipole configuration. Hereinafter we consider a GB disclination dipole produced by GB sliding, located near a triple junction of GBs and characterized by both the disclination strength ω and the arm (the distance between disclinations) p (Fig. 1a and b). The arm p in fact characterizes local plastic strain carried by GB sliding in the vicinity of the triple junction under consideration [17,19,38] (Fig. 1a and b).

(Note that GB sliding (Fig. 1b) is accommodated by emission of lattice dislocations from the triple junction A. Such a process was theoretically examined by Asaro and Suresh [44]. More precisely, Asaro and Suresh [44] considered the emission of partial and perfect dislocations or dislocation loops from a crack-like source produced by grain boundary sliding arrested at a triple junction. A theoretical analysis of the article [44] was focused on the initial stage of GB sliding, in which case p (the distance by which a triple junction shifts due to grain boundary sliding; see Fig. 1b) is around one crystal lattice parameter. Our further analysis will be focused on the stage at which severe GB sliding occurs, and the characteristic distance p is in the range from several crystal lattice parameters until the GB length.)

By analogy with micropipe formation at dislocations in semiconductors (e.g. [45–47]), we think that one of the channels for relaxation of stresses created by the disclination dipole is the formation of a nanoscale void (nanovoid), as shown in Fig. 1c. Another, competing way of evolution of the defect configuration under consideration is formation of a brittle nanoscale crack at the disclination dipole, as shown in Fig. 1d.

In general, the key difference between voids and brittle cracks is in both the rate of their formation and atomic rearrangements associated with their formation. Let us briefly discuss the difference in the exemplary situation with mode I cracks, which are the most widespread type of brittle cracks in solids. Formation of a mode I brittle crack occurs through very fast (momentary) displacements of its two surfaces in opposite directions normal to the surfaces, parallel to the applied force. The crack formation process is driven by a release of local stresses (and thereby elastic energy) at the crack surfaces and some of the local area near them. The formation of a void occurs through the comparatively slow, diffusion-controlled process of vacancy coagulation. The void formation process is driven by release of the elastic energy of an initially stressed local region, which disappears during the void formation. That is, the void formation is associated with the slow removal of atoms from the region where the void nucleates and grows, while brittle crack generation is associated with fast atomic displacements that break interatomic bonds. In the case under our consideration, voids and brittle cracks formed at disclination dipoles have slightly different locations. A nanovoid nucleates and grows in the region where the elastic energy density of a disclination dipole has its highest values, and the disclinations of the dipole are commonly located within this region (Fig. 1c). In so doing, as will be shown below, nanovoids tend to be sheet-like regions that grow at grain boundary interfaces and in their vicinities (Fig. 1e). A brittle crack forms at the surface where tensile stresses (normal to the surface) created by a disclination dipole are highest, and this surface is adjacent to one of the disclinations composing the dipole (Fig. 1d).

In general, the formation of a disclination dipole due to GB sliding and the formation of a void around such a dipole due to diffusional flow of vacancies require that both GB sliding and diffusion should be operative in the examined nanocrystalline solid. Since the diffusion-carried formation of nanovoids is a time-dependent process, it is sensitive to both the applied stress and the strain rate. In these circumstances, in practice, for any realistic value of the applied stress, one can find a strain rate range in which both grain boundary shearing and diffusional flow effectively operate in a material. Also, diffusional flow is greatly enhanced in nanocrystalline materials (because of large amount of grain boundaries specified by high diffusion coefficient) compared to coarse-grained polycrystals (where slow bulk diffusion commonly dominates). Therefore, the applied stress range in which the diffusional flow effectively operates (and can provide fast void formation and growth) in nanocrystalline materials is much wider than that in coarse-grained polycrystals.

Recently, a detailed study of the contributions of various deformation mechanisms in nanocrystalline solids to the total deformation was performed [48], using mesoscopic continuum modeling. Wei with co-authors showed that, for nanocrystalline Cu with a grain size of 30 nm at room temperature in the strain rate interval from 10^{-6} to 10^{-2} s^{-1}, the fraction of grain boundary sliding in the total deformation varies from 25% to 45%, while the fraction of grain boundary diffusional creep (Coble creep) varies from 40% to 50% [48]. Thus, at least, in nanocrystalline Cu, both grain boundary sliding and diffusional flow operate simultaneously in a wide range of strain rates and, as a rule, in a wide range of the applied stress. We assume that a similar situation takes place in nanocrystalline sapphire and nickel, which will be examined below.

Let us calculate the energy characteristics of the formation of an elliptic nanovoid with axes s and d (Fig. 1c) around the disclination dipole. The formation is characterized by the energy change $\Delta W = W_2 - W_1$, where W_1 is the energy of the initial (void-free) state (Fig. 1b) and W_2 is the

Author's personal copy

energy of the final state containing a nanovoid (Fig. 1c). The formation is energetically favorable if $\Delta W < 0$. The energy change ΔW (per unit disclination length) can be represented as the sum of three terms:

$$\Delta W = \Delta W_\Delta + W_s^e - W_{gb} \quad (1)$$

where ΔW_Δ is the change of the disclination dipole energy due to the nanovoid formation, W_s^e is the free surface energy of the elliptic nanovoid and W_{gb} is the energy of the GB fragments that disappear due to the nanovoid formation.

First, let us calculate the energy change ΔW_Δ of the disclination dipole due to the nanovoid formation. According to the theory of defects in solids, a disclination dipole with strength ω and arm (distance between the disclinations of the dipole) p is identical to a continuous uniform distribution of edge dislocations along the line connecting the dipole disclinations [49]. The total Burgers vector magnitude of the dislocation distribution is related to the dipole arm p and disclination strength ω by the equality [49] $B = 2p \tan \omega/2$ (Fig. 1a). In the conventional situation with low ω this equality is approximated well by the relation $B = \omega p$, which will be used in our following analysis. Since the stress field of a dislocation inside a void does not depend on its position within the void [50], the continuum distribution of dislocations inside the nanovoid is equivalent to a single dislocation (with the Burger vector $B = \omega p$) inside the nanovoid. In these circumstances, in calculation of the proper energy of the disclination dipole after the nanovoid formation, it is effective to use the known expression [51] for the proper energy W_{sd} of the corresponding superdislocation (with the Burgers vector $B = \omega p$) located within the nanovoid. The energy change ΔW_Δ of the disclination dipole due to the nanovoid formation can then be represented as the difference $\Delta W_\Delta = W_{sd} - W_\Delta^\infty$, where W_Δ^∞ is the energy of the disclination dipole in an infinite medium. Using the known expression for the energy of an edge dislocation inside an elliptic void [51] and the energy of a disclination dipole in an infinite medium [49], we find:

$$\Delta W_\Delta = -\frac{D\omega^2 p^2}{2}\left(\ln\frac{s+d}{4s} + \frac{s-d}{2(s+d)} + \frac{7-6\nu}{4(1-\nu)}\right) \quad (2)$$

where $D = G/[2\pi(1-\nu)]$, G is the shear modulus and ν is Poisson's ratio.

The free surface energy W_s of the cylinder nanovoid per its unit length can be written as:

$$W_s^e = 2s\gamma_s E\left(1 - \frac{d^2}{s^2}\right) \quad (3)$$

where γ_s is the specific (per unit area) energy of the free surface and $E(m) = \int_0^{\pi/2}(1 - m\sin^2\theta)^{1/2}d\theta$ is the complete elliptic integral of the second kind.

The energy W_{gb} of the GB fragments that disappear due to nanovoid formation, generally speaking, depends on the lengths and orientation of GBs adjacent to the disclination dipole. As a first approximation, we put

$$W_{gb} \approx \gamma_{gb} s \quad (4)$$

where γ_{gb} is the specific (per unit area) energy of the GB.

Formulas (1)–(4) allow one to calculate the energy change ΔW. With these formulas, we calculated the dependence of ΔW on the nanovoid sizes s and d in the scientifically and technologically interesting case of nanocrystalline ceramic α-Al_2O_3 (sapphire). In so doing, we used the following typical values of parameters of α-Al_2O_3 [52]: $G = 169$ GPa, $\nu = 0.23$, $\gamma = 1.5$ J m^{-2} [53], $\gamma_{gb} = 0.5$ J m^{-2} [53]. The contour maps of ΔW as functions of the nanovoid sizes s and d are shown in Fig. 2 for α-Al_2O_3, with $p = 5$ nm and $\omega = 15°$ (a) and 5° (b). As can be seen in the figure, in the case of $\omega = 15°$, when the void size s reaches the value of p, it is energetically favored to increase further (that is, ΔW decreases with increasing s) until it reaches the equilibrium size $s \approx 11$ nm. At the same time, ΔW decreases with decreasing d, so that the equilibrium value of d corresponds to $d \to 0$. In contrast, for $\omega = 5°$, ΔW increases with

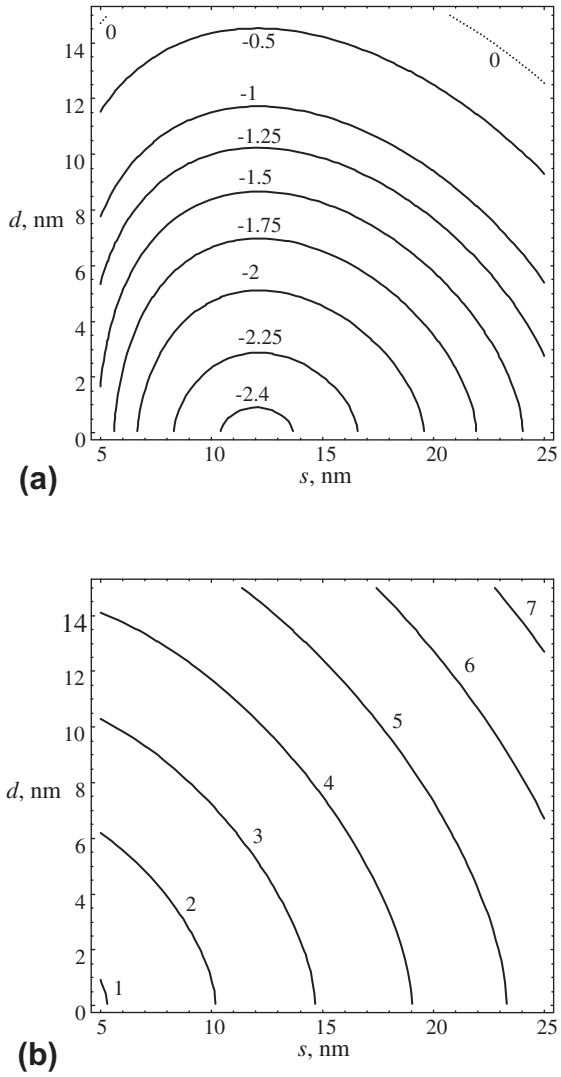

Fig. 2. Contour maps of the energy change ΔW due to the formation of an elliptic nanovoid in the coordinate space of the nanovoid dimensions s and d, for the case of α-Al_2O_3 and disclination strengths $\omega = 15°$ (a) and 5° (b).

Author's personal copy

increases in both s and d in the region $s \geqslant p$. In this case, the formation of a nanovoid around the disclination dipole is unfavorable. This is because, in the latter case, the dipole "power" ωp characterizing its stress field is too small to generate the nanovoid with the size $s \geqslant p$.

As follows from Fig. 2a, when the nanovoid forms, it tends to be very narrow, with $d \to 0$. However, the case of $d \to 0$ is evidently senseless. Hereafter we postulate that the minimum (physically reasonable) width of a nanovoid is $d = 1$ nm and consider a nanovoid with precisely such a width. (The value of $d = 1$ nm is close to typical values of GB width.) The equilibrium nanovoid length $s = s_e$ then follows from the relation $(\partial \Delta W/\partial s)|_{s=s_e} = 0$. The dependence of s_e on the parameter ωp for the case of α-Al_2O_3 and $d = 1$ nm is shown in Fig. 3. As can be seen in the figure, s_e increases with ωp. Therefore, the necessary condition for nanovoid formation, $s_e \geqslant p$, can be rewritten as $p \geqslant p_{np}$, where p_{np} is defined by the relation $s_e(\omega p_{np}) = p$ (see Fig. 3).

The dependence $p_{np}(\omega)$ for α-Al_2O_3 and $d = 1$ nm is shown in Fig. 4a. The formation of a nanovoid is favorable in the parameter plane (p, ω) region located above this curve and unfavorable in the region below it. The critical values p_{np} of the dipole arm (the minimum values at which the formation of a nanovoid around the disclination dipole is energetically favorable) are not very large. For example, for $\omega = 15°$, we have $p_{np} \approx 2$ nm.

3. Formation of nanoscale brittle cracks at grain boundaries with disclination dipoles in nanocrystalline materials

Now let us compare the conditions for the formation of an elliptic nanovoid around a disclination dipole (Fig. 1c) with the conditions for the formation of a brittle GB nanocrack at one of its disclinations (Fig. 1d). The condition for the crack advance in the situation shown in Fig. 1d can be written as (e.g. [17]) $q > q_c$, where $q_c = 16\pi(1-\nu)(2\gamma_s - \gamma_{gb})/(Gp\omega^2)$,

$$q = \tilde{l}\left(\frac{2\left(\sqrt{1+\tilde{l}}-1\right)}{\tilde{l}} - \ln\frac{\sqrt{1+\tilde{l}}+1}{\sqrt{1+\tilde{l}}-1}\right)^2 \qquad (5)$$

$\tilde{l} = l/p$ and l is the nanocrack length.

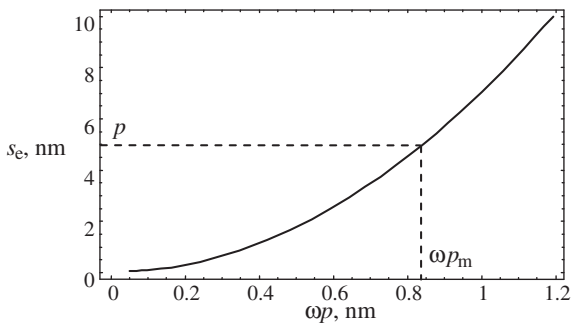

Fig. 3. Dependence of the equilibrium nanovoid size s_e on the parameter ωp for the case of α-Al_2O_3 and $d = 1$ nm.

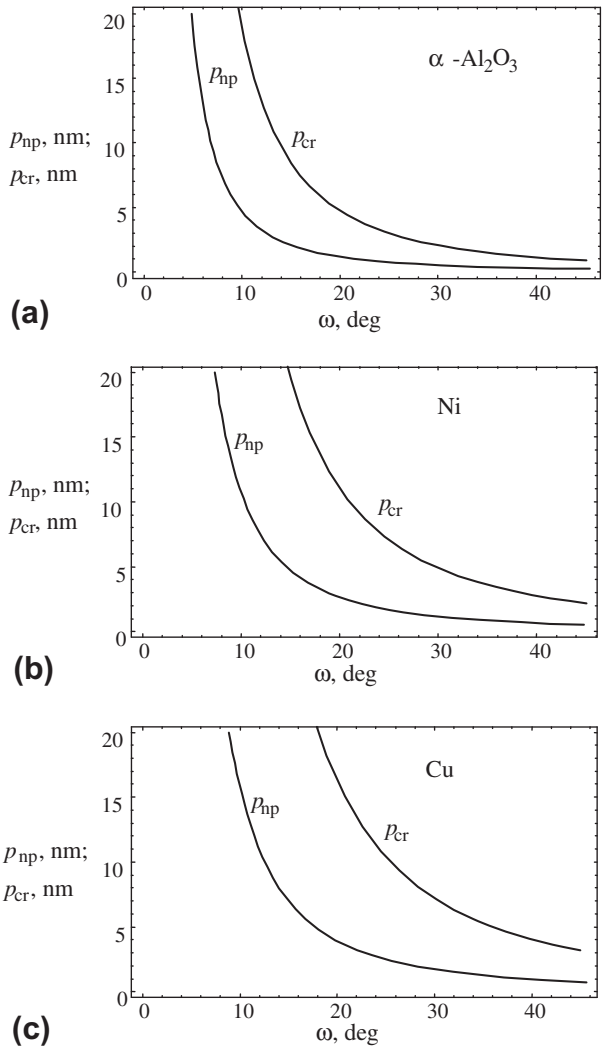

Fig. 4. Dependences of the critical (minimum) values of the dipole arm, p_{np} and p_{cr}, for the formation of a nanovoid and a nanocrack, respectively, on the dipole disclination strength ω in nanocrystalline α-Al_2O_3 (a), Ni (b) and Cu (c).

The dependence $q(\tilde{l})$ is shown in Fig. 5. The horizontal lines show two different exemplary values of q_c. As can be seen, two situations can take place, depending on the value of q_c. If the horizontal line showing the value of q_c lies higher than the maximum value of q_c, crack generation and growth are unfavorable at any crack length. In contrast, if the horizontal line showing the value of q_c lies lower than the maximum value of q_c, crack generation and growth are favored in some crack length interval $l_{e1} < l < l_{e2}$, where l_{e1} and l_{e2} are determined by the points of the intersection of the curve $q(\tilde{l})$ with the horizontal line (see Fig. 5). In the latter case, crack generation and growth in the interval $l < l_{e1}$ can occur through thermal fluctuations while its growth in the length interval $l_{e1} < l < l_{e2}$ occurs athermally. When the crack length reaches its equilibrium value l_{e2}, crack growth stops.

Let us denote the maximum value of the function $q(\tilde{l})$ as q_m ($q_m \approx 0.976$). Then the formation of a nanocrack occurs

Author's personal copy

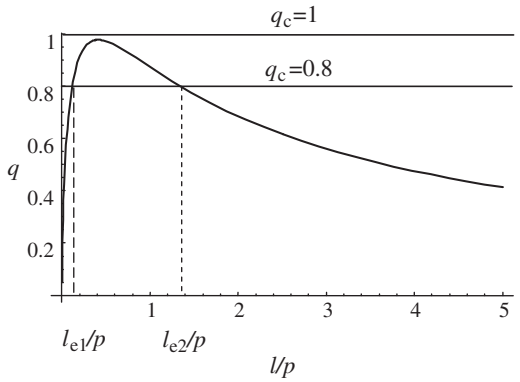

Fig. 5. Dependence of the parameter q on the normalized crack length l/p. The horizontal lines show two exemplary values of the parameter q_c. The quantities l_{e1} and l_{e2} denote the critical crack lengths between which crack advance is favored.

if $q_m > q_c$. Using the definition of q_c, the latter relation can be rewritten as $p > p_{cr}$, where $p_{cr} = 16\pi(1-\nu)(2\gamma_s - \gamma_{gb})/(q_m G\omega^2)$. The quantity p_{cr} specifies the minimum value of the dipole arm at a given value of ω at which crack formation at one side of the disclination dipole is energetically favorable. The dependence $p_{cr}(\omega)$ for α-Al_2O_3 is presented in Fig. 4a. The formation of a nanocrack is favorable in the region above this curve and unfavorable in the region below it. As follows from Fig. 4a, for any ω, $p_{cr} > p_{np}$, which means that the formation of a nanovoid around the dipole (Fig. 1c) is energetically favorable at lower degrees of local plastic strain carried by GB sliding (and characterized by the disclination dipole arm p) compared to those at which the formation of a nanocrack at one side of the disclination dipole (Fig. 1d) is energetically favorable. The difference between the values of p_{cr} and p_{np} is significant. For example, for $\omega = 15°$, we have $p_{np} \approx 2$ nm, whereas $p_{cr} \approx 8.6$ nm (Fig. 4a). Therefore, the formation of a nanovoid around a disclination dipole can be supposed to be more likely that the formation of a nanocrack at one side of the dipole.

In addition to the formation of nanovoids and nanocracks at GB disclination dipoles in nanocrystalline sapphire, we also analyzed their formation at GB disclination dipoles in nanocrystalline Ni and Cu. To do so, we used the following parameter values typical of Ni and Cu [27,54]: for Ni, $G = 73$ GPa, $\nu = 0.31$, $\gamma = 1.725$ J m^{-2}, $\gamma_b = 0.69$ J m^{-2}; for Cu, $G = 48$ GPa, $\nu = 0.34$, $\gamma = 1.725$ J m^{-2}, $\gamma_b = 0.65$ J m^{-2}. The analysis demonstrated a qualitative similarity between the cases of nanocrystalline sapphire and nanocrystalline Ni and Cu. In particular, as with the case of nanocrystalline sapphire, for a specified value of the disclination strength ω, the minimum dipole arm p_{np} for the formation of a nanovoids in nanocrystalline Ni and Cu is significantly smaller than the minimum dipole arm p_{cr} for the formation of a nanocrack (Fig. 4b and c). For example, in the case of Ni, for $\omega = 15°$ we have $p_{np} \approx 4$ nm, whereas $p_{cr} \approx 18$ nm (Fig. 4b). In the case of Cu, for $\omega = 15°$ we have $p_{np} \approx 7$ nm, whereas $p_{cr} \approx 29$ nm (Fig. 4c). As a consequence, the formation of nanovoids around disclination dipoles (Fig. 1c) in nanocrystalline metals (Ni and Cu) is more likely than the formation of nanocracks (Fig. 1d).

Though the dependences of the critical dipole arm on disclination strength for sapphire and metals (Fig. 4) are qualitatively similar, there is a significant quantitative difference in the values of the critical dipole arm between these materials. For instance, when the disclination strength ω is equal to 10°, the critical dipole arm p_{np} for void formation is around 5 nm in the case of sapphire (Fig. 4a) and around 11 nm in the case of nickel (Fig. 4b). When the disclination strength ω is equal to 20°, the critical dipole arm for crack formation is around 5 nm for sapphire (Fig. 4a) and around 11 nm for nickel (Fig. 4b).

4. Concluding remarks

Following the results of our theoretical analysis, the generation of nanovoids at triple junctions of GBs can effectively occur as an energetically favorable process driven by GB sliding in deformed nanocrystalline materials. Such nanovoids slowly nucleate in the stress fields of GB disclination dipoles formed at triple junctions due to GB sliding (Fig. 1a–c). According to our estimates, nanovoids tend to have elongated shapes, and their formation is more energetically preferred than that of brittle nanoscale cracks in deformed nanocrystalline Ni and Al_2O_3 (sapphire) in wide ranges of their parameters. (At the same time, generation of brittle nanoscale cracks is a rapid process that can be kinetically preferred compared to the slow, diffusion-controlled formation of nanovoids in nanocrystalline materials deformed at high strain rates.) Our theoretical model accounts for the experimental observations [1,33,34] of nanovoids at GBs and their triple junctions in deformed nanocrystalline Ni and Au. In the framework of the model, intense local plastic flow occurs through GB sliding and precedes the nanovoid formation. Their formation is a slow, diffusion-controlled process, and such nanovoids can serve as nuclei for viscous dimple rupture structures observed experimentally [1–7] at fracture surfaces of nanomaterials.

Large pile-ups of lattice dislocations – stress sources that often induce the generation of voids and brittle cracks in conventional coarse-grained polycrystals – are hardly formed in nanoscale grains of deformed nanocrystalline materials [23,31,32]. Therefore, the generation of nanovoids at GBs due to intergrain sliding could play the role of the dominant fracture process at the nanoscale level in nanocrystalline materials showing ductile fracture behavior. In this context, one can suggest the following schematic description of the experimentally observed [24,25] combination of macroscopically low plasticity and microscopically ductile fracture in nanocrystalline materials. Inhomogeneous deformation with plastic flow being localized in shear bands typically comes into play in nanocrystalline specimens (specified by low strain hardening and low strain rate sensitivity) under a tensile load [20,23].

Author's personal copy

Within such shear bands, GB sliding occurs intensively and produces nanovoids near triple junctions of GBs, as is theoretically demonstrated in this paper. Further development of GB sliding results in both the formation of mesoscopic sliding surfaces [55,56] – chains of GBs with approximately parallel planes – and the growth/elongation of triple junction nanovoids. The latter process causes the formation of dimpled fracture structures by interlinking nanovoids, as was previously suggested by Iwasaki et al. on the basis of their experimental data [25]. Mesoscopic sliding surfaces are commonly separated by grains or their clusters resistant to GB sliding, and each such surface typically consists of several GBs [55–57]. In the case discussed, the size of dimples formed by interlinking triple junction nanovoids at mesoscopic sliding surfaces should be close to the typical size of these surfaces (produced by GB sliding), that is, around several grain sizes. This statement is in a good agreement with the experimental measurements [24,25] of the sizes of dimples in nanocrystalline materials simultaneously showing macroscopically low plasticity and microscopically ductile fracture.

Finally, there is a situation where nanovoids are generated at GBs due to GB sliding in conventional microcrystalline materials, as with nanocrystalline materials. This situation represents superplastic deformation of microcrystalline materials, which involves both GB sliding and lattice dislocation slip as dominant deformation modes. Gouthama and Padmanabhan [30] recently reported on experimental observation of nanovoid nucleation at GBs in a microcrystalline copper alloy under superplastic deformation whose dominant deformation mode is GB sliding. These experimental data, and experimental observations of nanovoids at GBs and their triple junctions in deformed nanocrystalline metals [1,33,34], are indicative of a similarity between nanovoid nucleation processes in deformed nanocrystalline materials and superplastically deformed microcrystalline materials. In this context, the results of our theoretical model of nanovoid nucleation in nanocrystalline metals, presented in this paper, can also be relevant in a description of nanovoid nucleation in microcrystalline materials under superplastic deformation.

Acknowledgements

The work was supported, in part, by the Russian Academy of Sciences Program "Fundamental studies in nanotechnologies and nanomaterials", the National Science Foundation (Grant CMMI #0700272), the Russian Ministry of Science and Education (Contract 14.740.11.0353 and Grant NSh-3776.2010.1) and the Russian Foundation of Basic Research (Grant 08-01-00225-a).

References

[1] Kumar KS, Suresh S, Chisholm MF, Horton JA, Wang P. Acta Mater 2003;51:387.
[2] Li H, Ebrahimi F. Appl Phys Lett 2004;84:4307.
[3] Li H, Ebrahimi F. Adv Mater 2005;17:1969.
[4] Youssef K-M, Scattergood RO, Murty KL, Koch CC. Appl Phys Lett 2004;85:929.
[5] Cheng S, Ma E, Wang YM, Kecskes LJ, Youssef KM, Koch CC, et al. Acta Mater 2005;53:1521.
[6] Youssef KM, Scattergood RO, Murty KL, Koch CC. Scripta Mater 2006;54:251.
[7] Ebrahimi F, Liscano AJ, Kong D, Zhai Q, Li H. Rev Adv Mater Sci 2006;13:33.
[8] Moser B, Hanlon T, Kumar KS, Suresh S. Scripta Mater 2006;54:1151.
[9] Shan Z, Knapp JA, Follstaedt DM, Stach EA, Wiezorek JMK, Mao SX. Phys Rev Lett 2008;100:105502.
[10] Meirom RA, Clark T, Polcawich R, Pulskamp J, Dubey M, Muhlstein CL. Phys Rev Lett 2008;101:085503.
[11] Farkas D, Van Swygenhoven H, Derlet PM. Phys Rev B 2002;66:060101.
[12] Farkas D, Petegem S, Derlet PM, Van Swygenhoven H. Acta Mater 2005;53:3115.
[13] Mo Y, Szlufarska I. Appl Phys Lett 2007;90:181926.
[14] Farkas D, Willemann M, Hyde B. Phys Rev Lett 2005;94:165502.
[15] Ovid'ko IA, Sheinerman AG. Acta Mater 2004;52:1201.
[16] Ovid'ko IA, Sheinerman AG. Acta Mater 2005;53:1347.
[17] Ovid'ko IA, Sheinerman AG. Appl Phys Lett 2007;90:171927.
[18] Ovid'ko IA, Sheinerman AG, Aifantis EC. Acta Mater 2008;56:2718.
[19] Ovid'ko IA, Sheinerman AG. Acta Mater 2009;57:2217.
[20] Kumar KS, Suresh S, Van Swygenhoven H. Acta Mater 2003;51:5743.
[21] Ovid'ko IA. J Mater Sci 2007;42:1694.
[22] Padilla II HA, Boyce BK. Exp Mech 2010;50:5.
[23] Koch CC, Ovid'ko IA, Seal S, Veprek S. Structural nanocrystalline materials: fundamentals and applications. Cambridge: Cambridge University Press; 2007.
[24] Schwaiger R, Moser B, Dao M, Chollacoop N, Suresh S. Acta Mater 2003;51:5159.
[25] Iwasaki H, Higashi K, Nieh TG. Scripta Mater 2004;50:395.
[26] Hasnaoui A, Derlet PM, Swygenhoven H. Science 2003;300:1550.
[27] Hirth JP, Lothe J. Theory of dislocations. New York: Mc Graw-Hill; 1968.
[28] Armstrong RW. Metall Mater Trans A 1970;1:1169.
[29] Armstrong RW. In: Baker TN, editor. Yield, flow and fracture of polycrystals. Barking: Applied Science Publishers; 1983. p. 1–31.
[30] Gouthama, Padmanabhan KA. Scripta Mater 2003;49:761.
[31] Pande CS, Masumura RA, Armstrong RW. Nanostruct Mater 1993;2:323.
[32] Dao M, Lu L, Asaro RJ, De Hosson JTM, Ma E. Acta Mater 2007;55:4041.
[33] Milligan WW, Hackney SA, Ke M, Aifantis EC. Nanostruct Mater 1993;2:267.
[34] Ke M, Milligan WW, Hackney SA, Carsley JE, Aifantis EC. Nanostruct Mater 1995;5:689.
[35] Padmanabhan KA, Gleiter H. Mater Sci Eng A 2004;381:28.
[36] Mohamed FA, Chauhan M. Metall Mater Trans A 2006;37:3555.
[37] Mohamed FA. Metall Mater Trans A 2007;38:340.
[38] Ovid'ko IA, Sheinerman AG. Phys Rev B 2008;77:054109.
[39] Mukherjee AK. Mater Sci Eng A 2002;322:1.
[40] Bollmann W. Philos Mag A 1984;49:73.
[41] Bollmann W. Philos Mag A 1988;57:637.
[42] Romanov AE. Eur J Mech A 2003;22:727.
[43] Kleman M, Friedel J. Rev Mod Phys 2008;80:61.
[44] Asaro RJ, Suresh S. Acta Mater 2005;53:3369.
[45] Frank FC. Acta Cryst 1951;4:497.
[46] Huang XR, Dudley M, Vetter WM, Huang W, Wang S, Carter CH. Appl Phys Lett 1999;74:353.
[47] Ma X. J Appl Phys 2006;99:063513.
[48] Wei Y, Bower AF, Gao H. Acta Mater 2008;56:1741.
[49] Romanov AE, Vladimirov VI. In: Nabarro FRN, editor. Dislocations in solids, vol. 9. Amsterdam: North-Holland; 1992. p. 191–302.

Author's personal copy

[50] Eshelby JD. In: Nabarro FRN, editor. Dislocations in solids, vol. 1. Amsterdam: North-Holland; 1980. p. 167–222.
[51] Ovid'ko IA, Sheinerman AG. Philos Mag 2006;86:1415.
[52] Munro RG. J Am Ceram Soc 1997;80:1919.
[53] Watanabe T, Yoshida H, Saito T, Yamamoto T, Ikuhara Y, Sakuma T. Mater Sci Forum 1999;304–306:601.
[54] Smithells CJ, Brands EA. Metals reference book. London: Butterworths; 1976.
[55] Sergueeva A, Mukherjee AK. Rev Adv Mater Sci 2006;13:1.
[56] Sergueeva A, Mara NA, Krasilnikov NA, Valiev RZ, Mukherjee AK. Philos Mag 2006;86:5797.
[57] Bobylev SV, Mukherjee AK, Ovid'ko IA. Rev Adv Mater Sci 2009;19:103.